Fourth Year Project Report

Relay Feedback Models of Biologial Oscillators

Rajiv Kurien

Queens' College

2015-2016

Technical Abstract

Biological behaviours are complex, rich and varied. Oscillations in biology are diverse and models replicating them are often high dimensional and nonlinear. These models quickly get difficult to analyse and do not have a generalised theory (except two dimensional systems) to predict existence of oscillations, stability and time periods. However, the theory of relay feedback systems, a very particular type of nonlinear feedback, used classically in automatic control, has analytical solutions to these questions.

The aim of this project was to elucidate how useful the theory of relay feedback systems would be to analysing biological oscillations. As a first step, the basic model of relay feedback was applied to two classical biological models — the Goodwin oscillator model for genetic oscillations and the FitzHugh-Nagumo model for action potentials. Relay feedback was able to simulate oscillations in these models, reflecting upon how biological oscillations often incorporate digital and analogue dynamics.

As a second step, the potential of nested relay feedback to model complex oscillations was investigated. A normal form model of neuronal bursting was dissected as two interconnected relay feedback systems. The Hindmarsh-Rose model of neuronal bursting was then shown to have the same structure as the normal form model, conceding it to be modelled by relay feedback.

The project revealed how relay feedback provides an appealing modelling framework for the analysis of quantitative models of biological oscillations. It highlights how biological models can be viewed as an interconnection of analogue (L.T.I) and digitial (relay) logic. Due to the theory of relay feedback oscillations being tractable in high dimensions, it provides a way to analysing high order biological models and is amenable to robustness and sensitivy analysis.

Contents

1   Introduction

Oscillations are an integral component in the world around us. Biochemical and biophysical rhythms are ubiquitous charactereristics of living organisms, from rapid oscillations of membrane potential in nerve cells to slow cycles of ovulation in mammals [1]. Understanding the molecular and cellular mechanisms responsible for oscillations is crucial for unravelling the dynamics of life[2]. Fundamentally, oscillations are due to feedback, and classical control has usually been applied to reduce these oscillations. With the pursuit of understanding biological oscillations, feedback models have been explored to understand how to generate different types of oscillations. Such research aims to yield a better understanding of how biology works, giving us tools to engineer biology to suit our needs.

Several models of biological oscillations display logic. Gene regulatory models incorporate a gene turning on or off. Neuronal models are excitatory, displaying oscillations when a threshold is exceeded. Such biological models of oscillations inherently combine analogue and digital signals. They may have a large number of parameters that require tuning in order to produce oscillations and pose difficulties in extracting useful information about the effect of these parameters on existence of oscillations and their frequency. Figure 1 shows how for a three variable dynamical system, changing two parameters reveals a rich repertoire of oscillatory behaviours. A method of addressing models of oscillations described in [2], simply amounts to simulating the system around the parameter space that is available or in a physiological range.For high dimensional systems, a parameter search approach is computationally expensive. Furthermore, this does not easily predict the frequency of oscillations.
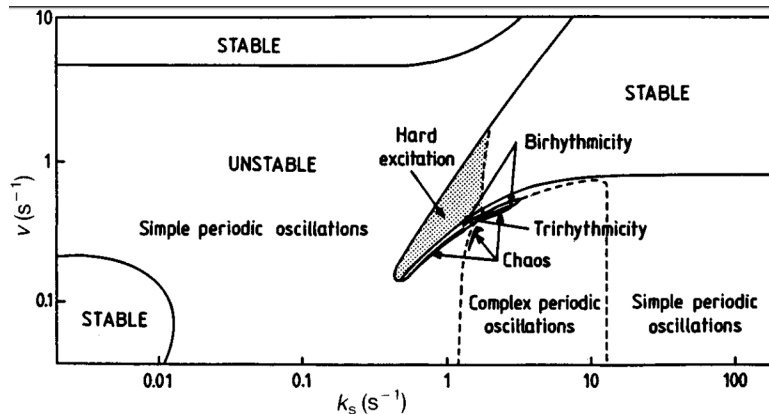

Figure 1: Different domains of dynamic behaviour in the parameter space $v - k_s$ for a three variable multiply regulated biochemical system. Source [3].

Another method of tackling this issue is to model oscillations as adaptation around a static nonlinearity. This approach links biological oscillation to a methodology developed in classical control — relay feedback systems, which gives us tools to analyse oscillations.

Relay feedback consists of a plant connected via negative feedback to a static hysteretic nonlinearity called a relay. Relay feedback is most popularly used in automatic tuning of PID controllers. It is one of the simplest and most robust auto-tuning techniques for process controllers and has been successfully applied to industry for more than 15 years [4]. Oscillations in simple relay feedback

systems have been well understood and have analytical results even for high dimensional systems.

Consequently, this raises the question: Are relay feedback models appropriate to analyse biologial oscillations?

This project starts to addresses this question, and the report is structured as follows. In section 2, some of the analytical results for oscillations in relay feedback systems from [5] is presented. Section 3 uses a simple relay feedback system to model continous oscillations in the Goodwin and FitzHugh-Nagumo models. Finally, section 4 investigates using two coupled relay feedback systems to model a complex oscillation — bursting, and consequently the famous Hindmarsh-Rose model for neuronal bursting.

2 Theory

A relay is a particular type of nonlinearity that has only two output values, a high or a low value, dependent on the input. Figure 2 shows a symmetric relay element that satisfies the input (e) and output (u) relationship:

$$u(t) = \begin{cases} d \text{ if } e > \epsilon \text{ or } (e > -\epsilon \text{ and } u(t-) = d) \\ -d \text{ if } e < -\epsilon \text{ or } (e < \epsilon \text{ and } u(t-) = -d) \end{cases} \tag{1}$$
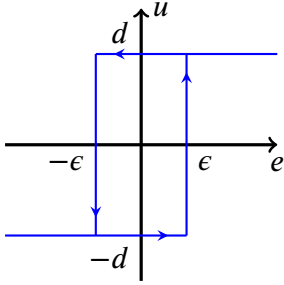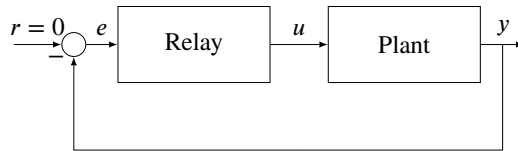

Figure 2: Relay element   Figure 3: Relay feedback

Figure 3 reveals how a typical relay feedback system is connected. The output of a plant (y), is connected to the relay ($e = -y$), and the output of the relay is input to the plant. Relay feedback systems tend to cause oscillations as the plant is subjected to maximal input (high or low) in the opposite direction when the plant exceeds a threshold (ϵ or $-\epsilon$), as shown in Figure 4.

Relay feedback systems combine analogue and digital signals, which is reminiscent of switching behaviour in biological oscillations.
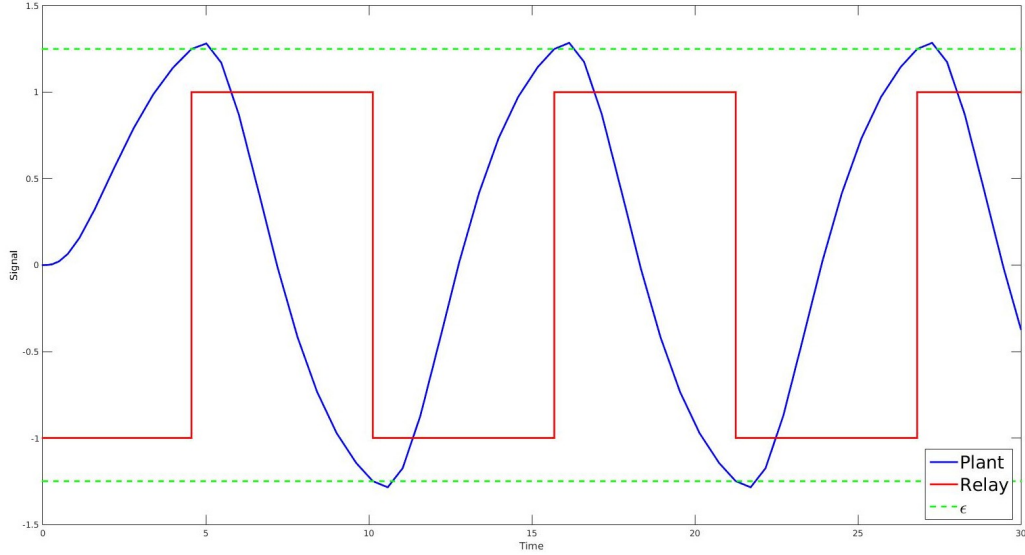
Figure 4: Oscillations in a relay feedback system. The relay switches when the plant reaches the hysteresis limits $\pm\epsilon$, causing the plant to oscillate between those limits.

2.1 Symmetric oscillations

Consider the linear time invariant system:

$$\begin{aligned}\dot{x} &= Ax + Bu \\ y &= Cx\end{aligned} \tag{2}$$

When this system is connected to the relay (1), with $e = -y$, the system can have a symmetric limit cycle of period $T = 2h$ if the following condition is met:

$$C(I + e^{Ah})^{-1} \int_0^h e^{As} B \mathrm{d}s = \frac{\epsilon}{d} \tag{3}$$

This theorem is able to deal with high dimensional systems, giving a general approach to analysing nonlinear models of oscillations.

2.2 Asymmetric oscillations

When the relay is characterized by:

$$u(t) = \begin{cases} d_1 \text{ if } e > \epsilon \text{ or } (e > -\epsilon \text{ and } u(t-) = d_1) \\ -d_2 \text{ if } e < -\epsilon \text{ or } (e < \epsilon \text{ and } u(t-) = -d_2) \end{cases} \tag{4}$$

The LTI system given by (2) can have asymmetric oscillations when $e = -y$ and the following conditions for a limit cycle with period T are met:

$$\begin{cases} C(I - \Phi)^{-1}(\Phi_2\Gamma_1 d_1 - \Gamma_2 d_2) = -\epsilon \\ C(I - \Phi)^{-1}(-\Phi_1\Gamma_2 d_2 + \Gamma_1 d_1) = \epsilon \end{cases} \tag{5}$$

5

where

$$\Phi = e^{AT} , \Phi_1 = e^{A\tau} , \Phi_2 = e^{A(T-\tau)}$$

$$\Phi_1 = \int_0^\tau e^{As} \mathrm{d}s B , \Gamma_2 = \int_0^{T-\tau} e^{As} \mathrm{d}s B \tag{6}$$

The asymmetric oscillation is split into two parts, a period when the relay output is low, τ and the period when the relay output is high, $T - \tau$, as shown in Figure 5.
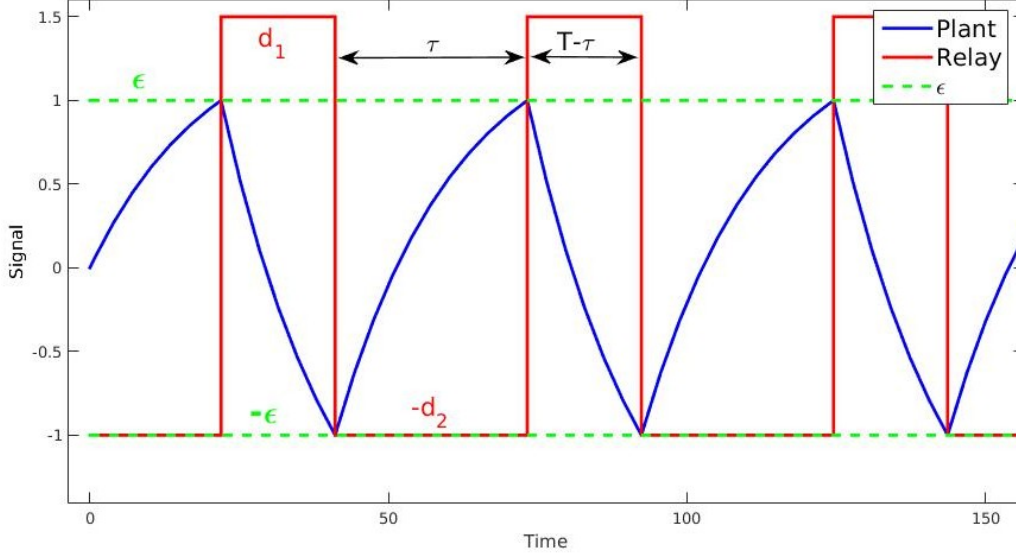

Figure 5: Asymmetric oscillations with relay feedback.

In this project, once a model was approximated using relay feedback, the tools stated above were used to predict the existence of limit cycles and their time periods. Parameters of a model could be varied and their effect understood by the above equations. [5] also derived initial conditions for these oscillations and how to check the local stability of the oscillations, which again were used to analyse each model.

3   Relay feedback models of fundamental biological limit cycles

Two fundamental models of continuous oscillations in biology will be modelled as simple relay feedback systems in this section. This proof of concept step reveals the use of relay feedback in order to predict time periods of oscillations and understanding how different parameters affect oscillations.

3.1   Goodwin oscillator model

The Goodwin oscillator is a biochemical oscillator model based on negative feedback alone. This genetic oscillator describes the conceptual mechanism of how mRNA, protein and end product interact.

Written in their non-dimensional form [1], the Goodwin oscillator's kinetic equations are:

$$\frac{dx_1}{dt'} = \frac{1}{1 + x_3^p} - b_1 x_1 \tag{7}$$

$$\frac{dx_2}{dt'} = b_2(x_1 - x_2) \tag{8}$$

$$\frac{dx_3}{dt'} = b_3(x_2 - x_3) \tag{9}$$

where x_1, x_2, x_3 are non-dimensionalised concentrations of mRNA, protein and end product, respectively. The only nonlinearity, ($\frac{1}{1+x_3^p}$), becomes a relay with no hysteresis as $p \to \infty$ (see Figure 6).
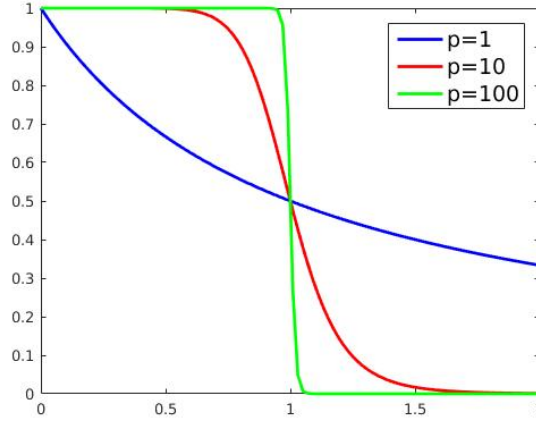

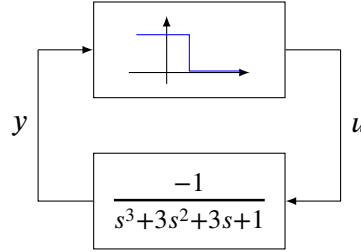Figure 6: Nonlinearity becomes a relay with no hysteresis, as $p \to \infty$.

Figure 7: Relay feedback system model of Goodwin oscillator ($b_1 = b_2 = b_3 = 1$).

Setting $b_1 = b_2 = b_3 = 1$ (for simplicity) and rewriting the equations such that the linear equations form the plant and the nonlinearity is a relay, results in the system shown in Figure 7 with state space realisation:

$$\dot{x} = \begin{bmatrix} -1 & 0 & 0 \\ 1 & -1 & 0 \\ 0 & 1 & -1 \end{bmatrix} x + \begin{bmatrix} 1 \\ 0 \\ 0 \end{bmatrix} u \tag{10}$$

$$y = \begin{bmatrix} 0 & 0 & 1 \end{bmatrix} u \tag{11}$$

$$u = \begin{cases} 0 \text{ if } e \geq 1) \\ 1 \text{ if } e < 1) \end{cases} \tag{12}$$

7

Using the theory for asymmetric oscillations, initial conditions were derived numerically. The limit cycle with the appropriate time period was shown to be locally stable and the simulations of the Goodwin model (with a large p) and the relay feedback model were very similar (see Figure 8). This (novel) use of relay feedback systems to model biological oscillations is a link between classical control theory and biological models. The relay feedback model of gene dynamics explicitly models the logic of a gene turning off/on, and gives new insight into understanding these oscillations. This framework gives us a methodology to approach high-dimensional models of circadian rhythms, such as the 10 dimensional model for circadian oscillations in *Drosophila* [7].
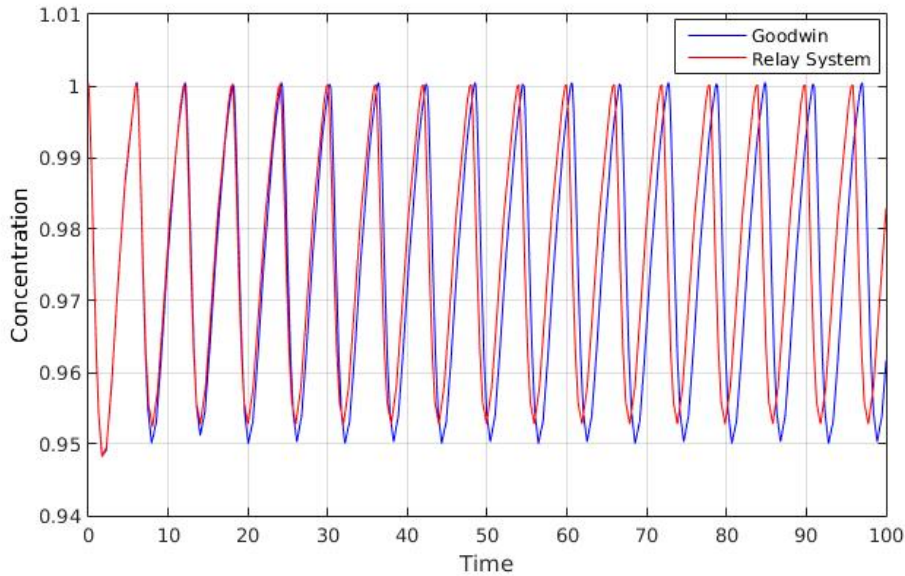

Figure 8: Relay system models Goodwin oscillator well as $p \to \infty$.
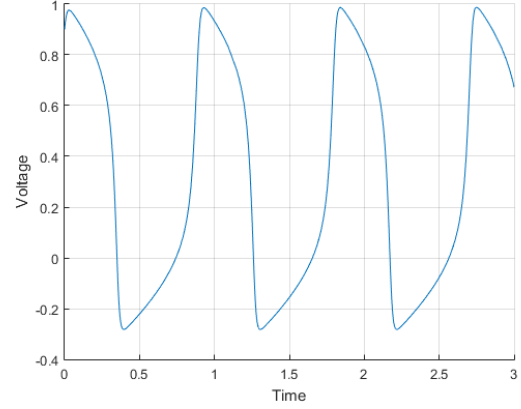
3.2 FitzHugh-Nagumo model

In this section, the use of relay feedback systems is extended to model a system where the relay is not as 'obvious', as was in the previous section.

3.2.1 Introduction

The Hodgkin-Huxley model[8] was the first quantitative model of the propagation of an electrical signal along a squid giant axon [6]. It is considered as one of the most important mathematical models in all of the physiological literature [6], and led to the study of excitable systems. The FitzHugh-Nagumo model simplifies the Hodgkin-Huxley model (of four variables) in terms of two variables, one fast and one slow. The FitzHugh-Nagumo model exhibits as clearly as possible the basic dynamic interrelationships between the variables of state which are responsible for the properties of threshold, refractoriness, and finite and infinite trains of impulses[9]. With the fast variable, v, representing the
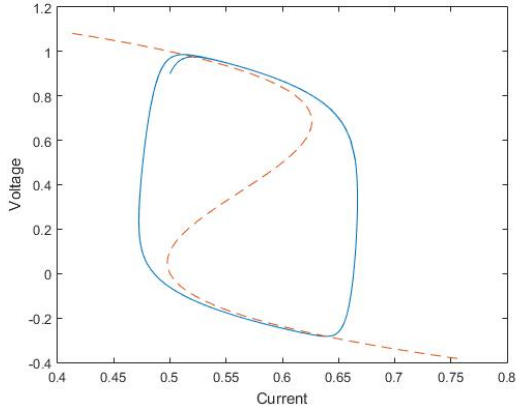
(a) Phase portrait. The cubic null-
cline is shown as the dashed line.

(b) Voltage oscillations.

Figure 9: Continous oscillations in the FitzHugh-Nagumo model.

voltage and the slow variable, w, representing the current, the FitzHugh-Nagumo model is:

$$\epsilon \dot{v} = f(v) - w + I_{app} \tag{13}$$

$$\dot{w} = v - \gamma w \tag{14}$$

where:

$$\epsilon \ll 1 \text{ and } f(v) = v(1 - v)(v - \alpha) , 0 < \alpha < 1.$$

I_{app} is the externally applied current (representing the stimulus). The nullclines[1] of the fast and slow variables have a cubic shape and a linear shape respectively. The input current, I_{app}, shifts the cubic nullcline, affecting where the nullclines intersect, i.e the equilibrium points. For certain input currents, the nullclines intersect at only one (unstable) point and cause continous oscillations. With $\alpha = 0.1, \gamma = 0.5, \epsilon = 0.01$ and $I_{app} = 0.5$, the uniqure rest point is unstable. Since $\epsilon \ll 1$, the fast variable tries to follow the stable branches of the cubic nullcline where possible and then quickly jumps to the other stable branch. That is the voltage stays at a high value for some time and then quickly jumps to a low value and then jumps up to a high value (see Figure 9). Meanwhile, the current slowly adapts to the high/low value of the voltage, pushing the system to leave the stable branches eventually. The behaviour of the system in the phase plane follows from singular perturbation theory[6].

3.2.2 Converting to relay feedback model

As $\epsilon \to 0$, the phase portrait of the voltage and current becomes more and more linear and closely resembles a rotated relay with hysteresis (Figure 10). This can be understood as high gain inversion [10], and the voltage behaves like the ouput of a skewed relay. So, when the system is continuously oscillating, it allows us to replace the cubic nullcline with a skewed relay (see Figure 11b).

---

[1]The nullcline is the line along which a variable's time derivative is zero
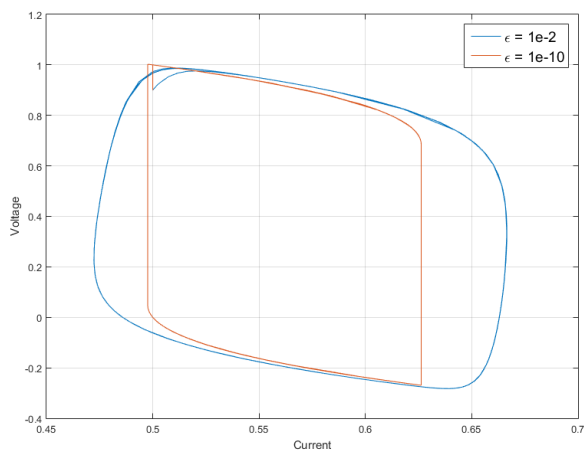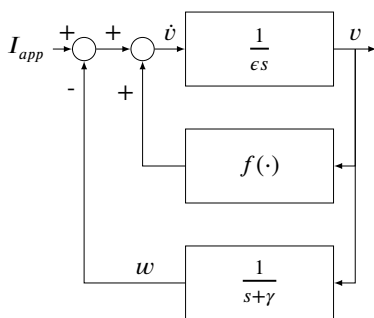
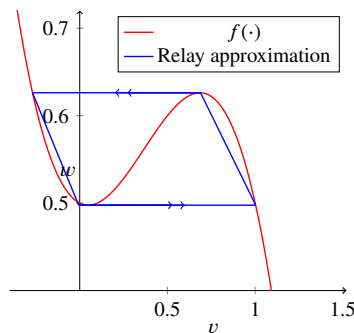(a) Phase portrait. Hysteresis be-
comes more linear and 'relay'.
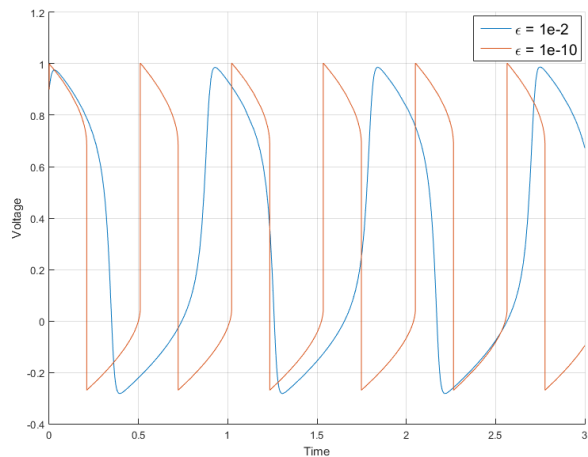
(b) Voltage oscillations become more
'discrete', similar to a relay ouput.

Figure 10: In the limit $\epsilon \to 0$, the voltage ouput looks like the output of a relay. The hysteresis looks like a skewed relay.

(a) Block diagram

(b) Nonlinearity and the "relay" ap-
proximation

Figure 11: FitzHugh-Nagumo model.

High gain inversion

$$0 = f(v) - w + I_{\text{app}} \tag{15}$$

$$v = f^{-1}\left(w - I_{\text{app}}\right) \tag{16}$$

$$v \approx \text{Relay}(w) \tag{17}$$

This allows us to replace the inner loop in 11a. With a shift in co-ordinates to make the 'relay' symmetric about the orgin, and a change of basis so that an unskewed relay can be used, results in the relay feedback system in Figure 12. Details of this transformation are illustrated in the Appendix. Now, using equation (3), we can derive the time period of the oscillation and its local stability. The results are shown in Figure 13. The relay feedback model matches the oscillations very closely.

This model reveals how the oscillations can be understood as adaptation around a hysteresis. The current slowly adapts to each change in voltage, around the relay hysteresis, causes the voltage to oscillate.
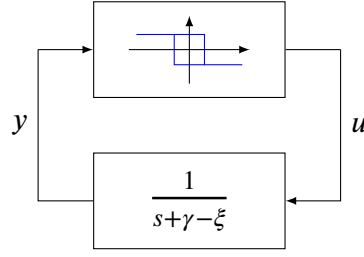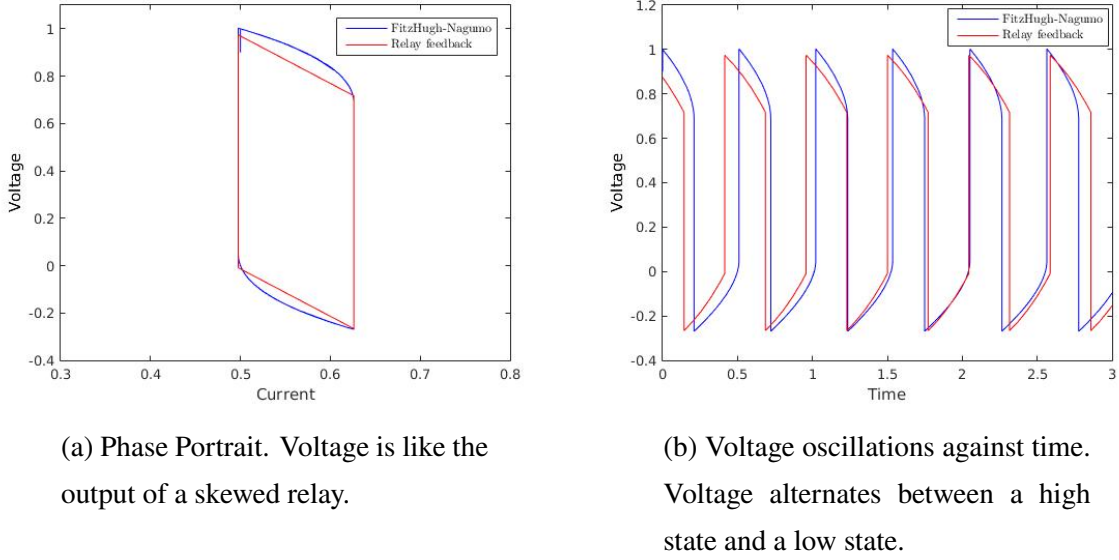
10

Figure 12: Relay feedback model of FitzHugh-Nagumo.

(a) Phase Portrait. Voltage is like the output of a skewed relay.

(b) Voltage oscillations against time. Voltage alternates between a high state and a low state.

Figure 13: FitzHugh-Nagumo model and Relay feedback model match in $\lim_{\epsilon \to 0}$

4 Relay feedback model of nested oscillations

In the previous section, the use of the relay feedback framework for analysing simple oscillations was found to very useful. Now the question arises as to whether this framework is capable of tackling complex oscillations. Bursting, a complex oscillation, can be understood as the interaction between two excitable systems with different time scales[14]. In other words, it can be understood as two coupled FitzHugh-Nagumo models. In this section,

In this section, a normal form model of bursting is introduced and then simplified into two

In this section, the application of the use of relay feedback analysis is extended to a more complex biological oscillation — bursting. Bursting can be understood . This research step, show A bursting model's nonlinearities are simplifed to piecewise-linear non-linearites and a separation of time scales approach is used to decompose the two coupled oscillators.

4.1 Bursting

Bursting is an important signaling component of neurons, characterized by a periodic alternation of bursts (periods of rapid oscillatory activity) and quiescent (membrane potential changes slowly)periods [12]. Bursting observed in cells can have a wide variety of periods, ranging from a few seconds to a

11

few minutes [6]. This general phenomenon is believed to play an important role in several signalling mechanisms. Bursting can also be viewed as a two state automaton in frequency [14]; encoding memory into four states– resting, fast oscillations, slow oscillations and bursting.

All neuronal bursters have three distinct time scales: a fast time-scale for spike generation, a slow time-scale for the intraburst spike frequency, and an ultra slow time-scale for the inter burst frequency[12].

This separation of timescales is used to decompose bursting into two coupled relay feedback systems. As a first step, a bursting model normal form from [11] is introduced. Then, the nonlinearites are simplified and finally, the three different time scales are separated out to reduce the model into relay feedback systems.

4.2 A three-time scale bursting normal form

The three-time scale bursting normal form organized by the winged cusp is presented in [11]. It is based on unfolding of the organizing center called the winged cusp to obtain a finite family distinct,robust static behaviours [11]. The model is based on Singularity theory and the interested reader is referred to [11] for a comprehensive exposition of how this model realises a variety of nonlinear behaviours.

The fundamental basis for this model is the robust co-existence of a stable fixed point and a stable relaxation limit cycle as shown in Figure 14. The stable limit cycle is similar to the FitzHugh-Nagumo model's phase portrait. This model generalizes FitzHugh-Nagumo by adding a third variable (ultra-slow) in negative feedback, which adapts in the dimension normal to the phase portrait (see Figure 15). The basic idea is that there are slow processes which modulate the faster spike generating dynamics [13]. The ultra-slow adaptation switches the behaviour between spiking and resting. The state-space equations for this model is:

$$
\begin{aligned}
\epsilon_f \dot{x}_f &= -x_f + S\left(x_f + B_\delta\left(u + x_s + \tfrac{\gamma}{2}x_f\right) + \beta x_f + \alpha - x_{us}\right) \\
\dot{x}_s &= x_f - x_s \\
\dot{x}_{us} &= \epsilon_u\left(-x_{us} + k_u(x_f + \bar{x}_u)\right)
\end{aligned}
\tag{18}
$$

where:

$$
\begin{aligned}
&\text{Sigmoid nonlinearity: } S(u) = \tanh(u) \\
&\text{Bump nonlinearity: } B_\delta(u) := S(u + \delta) - S(u - \delta) - 2S(\delta), \quad \delta \neq 0
\end{aligned}
\tag{19}
$$

The block diagram for this circuit is shown in Figure 16. Typical bursting is shown in Figure 17 where the ultra-slow variable modulates the behaviour.

4.2.1 The adaptation parameter for the ultra-slow negative feedback loop

The (unfolding) parameter α modulates monotonically the winged-cusp singularity[11], as shown in Figure 18. The bursting model thus relies on continously adapting this parameter, using the ultra-slow variable, around the bistable range. As x_{us} reaches its maximum value, the nullclines of the fast
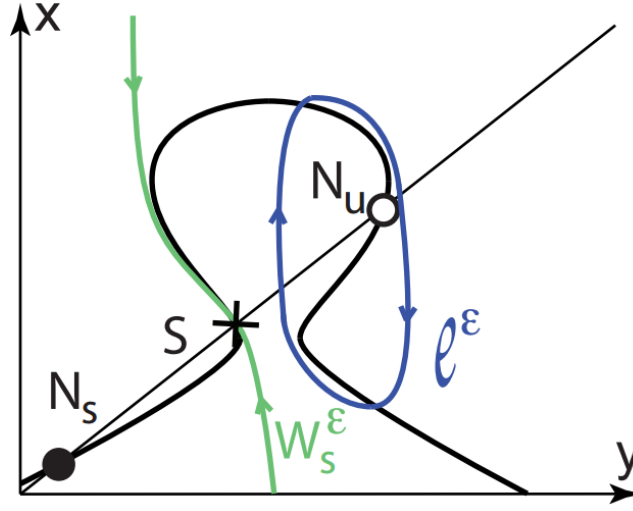
Figure 14: Phase portrait (qualitative) of the three-time scale bursting normal form. N_s is the stable equilibrium, N_u is the unstable equilibrium, S is the saddle point, W_s^ϵ is the stable manifold of S and l^ϵ is a stable limit cycle. The thick black line is the fast variable's nullcline, known as the mirrored hysteresis (winged cusp singularity) and the slow variable's nullcline is the thin straight line. Source [12].
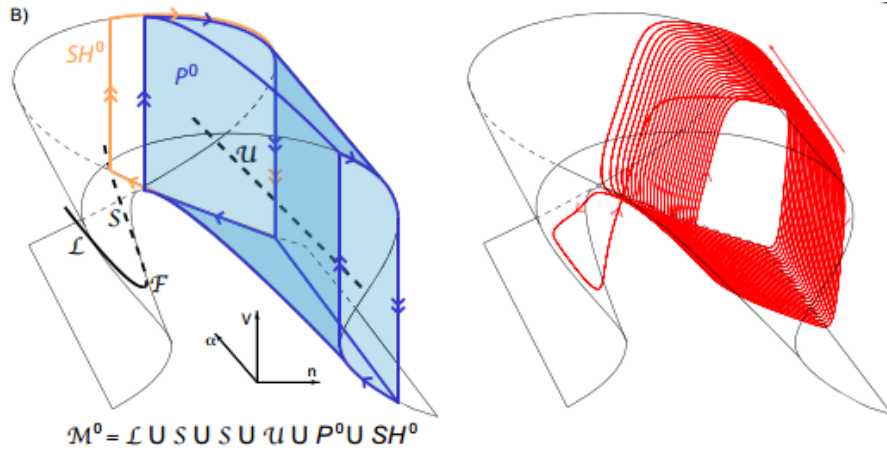

Figure 15: Three-dimensional singular invariant set $\mathcal{M}^0$ (left), which provides a skeleton for a three-time scale bursting attractor (right). The ultra-slow parameter adapts to swtich the system from spiking to resting and vice versa. See [12] Figure 4 for details. Source [12].

and slow variables will only intersect at the stable fixed point (low x_f). This drives the system to the quiescent period, while x_{us} slowly recovers. When x_{us} reaches its minimum value, the nullclines of the fast and slow variables will only intersect at a high x_{us} which then becomes the unstable fixed point as x_{us} recovers. This drives the system to the spiking period. It is clear now that the ultra-slow parameter can be modelled as a relay feedback system, oscillating around the bistable range. However, due to the bump nonlinearity, the slow and fast systems need some more dissection before it can be modelled as a relay feedback system.
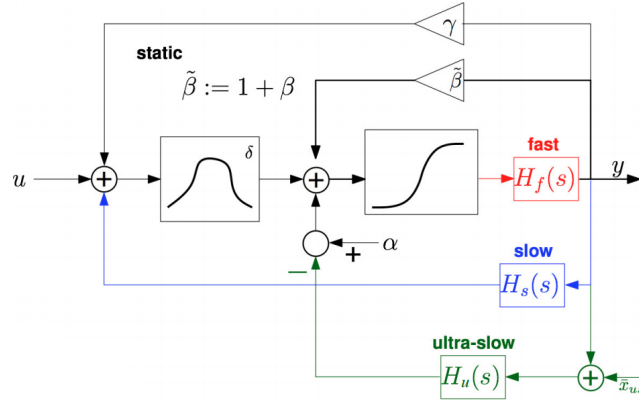
Figure 16: Three-time scale bursting normal form block diagram. Source [11].
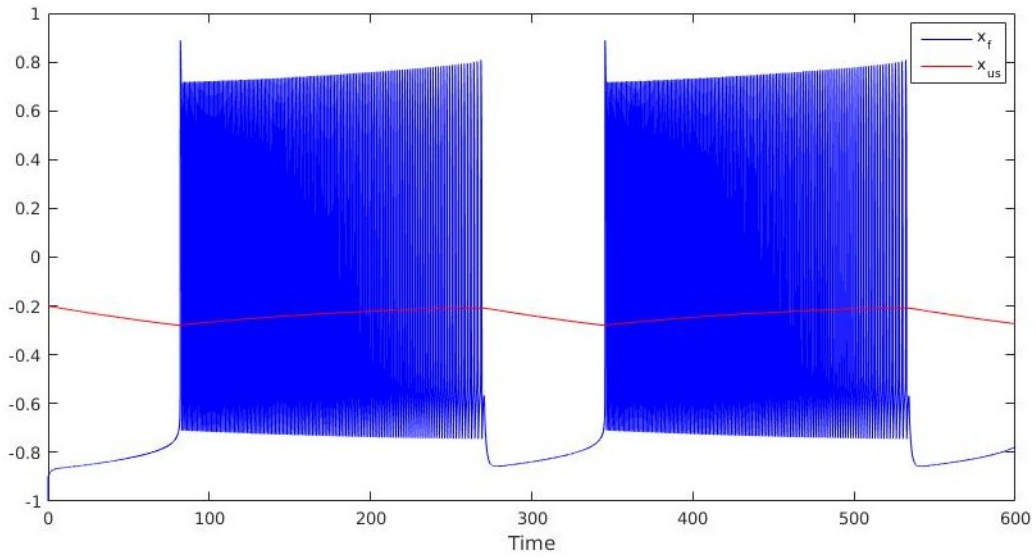

Figure 17: Bursting. The ultra-slow oscillations of the x_{us} switches the output x_f between spiking and resting.
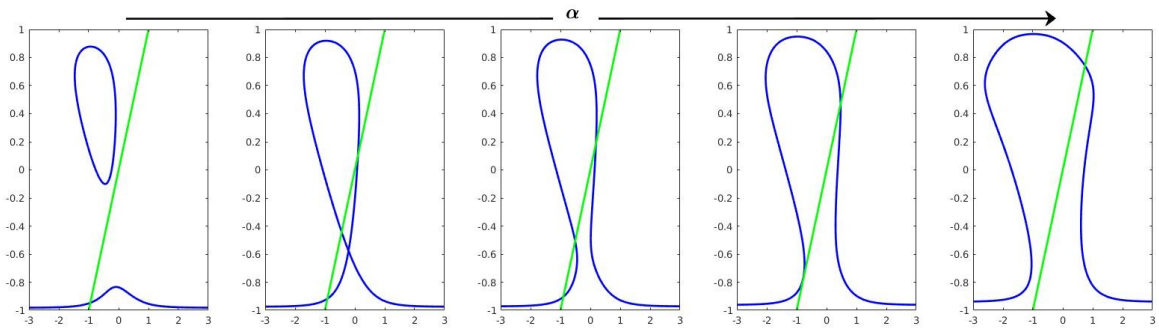

Figure 18: Fast nullcline changing as α increases. Within a fixed range of α, the system has both the resting and the spiking equilibrium. This is the bistable range.

14

4.2.2 The positve feedback in fast inner loop

The positive feedback of the fast plant around the sigmoidal nonlinearity creates a nonlinearity with hysteresis. This can be understood by considering positive feedback for a saturation function, shown in Figure 19. By assuming that x_f is much faster than the other variables, we can clearly approximate the positve feedback loop as a relay. This is equivalent to $\epsilon_f \to 0$, which was done earlier for the FitzHugh-Nagumo model.

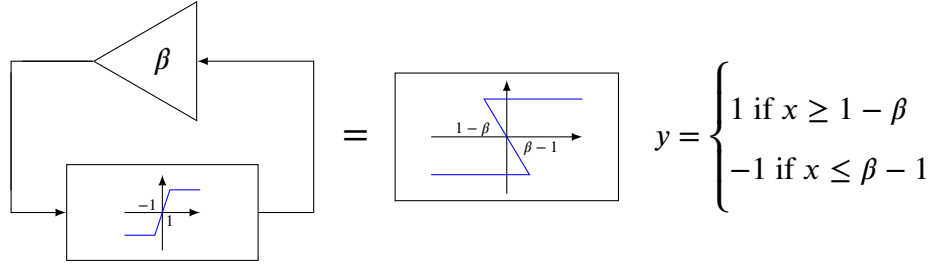Figure 19: For the saturation function, for $\beta > 1$, the nonlinearity gains a hysteresis of width 2β.

4.2.3 The bump nonlinearity

The bump nonlinearity (Figure 20) affects what kind of feedback the slow plant provides. When the system is spiking, the input to the bump is always greater than zero. This means the system was in the regime where the bump had a negative gradient. The bump provided negative feedback, causing the slow plant to adapt around the hysteresis of the sigmoid nonlinearity. That is, when spiking, the model essentially simplifies down to the FitzHugh-Nagumo model during continous oscillations. However, when the model was quiescent, the input to the bump was negative. The bump provided positive feedback, driving the system to the stable equilibrium.

Now it is required to simplify this model in order to allow us to use the analytical results for relay feedback systems.
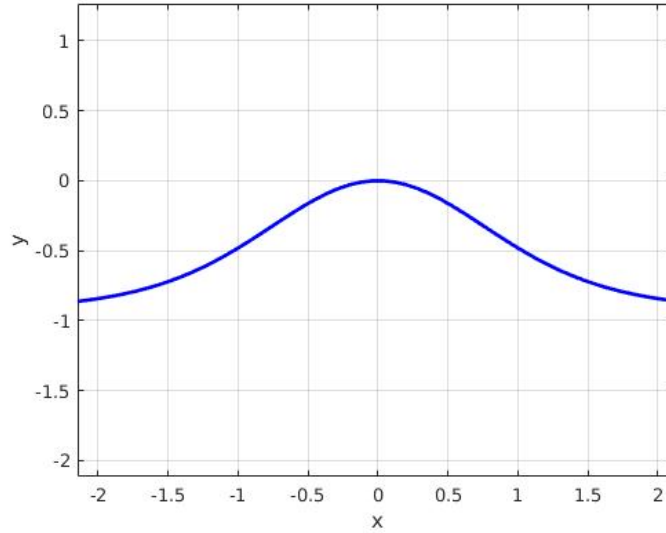
Figure 20: Bump nonlinearity

4.2.4 Using piece-wise linear non-linearities

As shown in 21, the saturation function is a good approximation to the sigmoidal nonlinearity. Furthermore, since the positive feedback gain is $\tilde{\beta} := 1 + \beta$, this can be replaced by a positive feedback of just β around a relay with no hsyteresis. The is then equivalent to a relay with hysteresis limits $\pm\beta$.

The bump nonlinearity with δ set to 0.5, can be approximated by the piecewise linear function shown in Figure 22. The piecewise linear function simplifies the model very nicely since the positive/negative feedback gain is constant. The function is:

$$B := \begin{cases} \frac{1}{2}x & \text{if } -2 < x < 0 \\ -\frac{1}{2}x & \text{if } 0 < x < 2 \\ -1 & \text{otherwise} \end{cases} \tag{20}$$

The system's phase portrait is shown in Figure 23. The new fast nullcline approximates the original nullcline.

4.2.5 Separation of time scales to separate into relay feedback systems

By assuming that the fast variable changes instantaneously ($e_f \to 0$), the innermost loop involving the fast plant H_f can be replaced by a relay with hysteresis (Figure 24).

While the system is spiking, the bump nonlinearity can be replaced by a constant gain providing negative feedback. Furthermore, Figure 27 shows how the ultra slow variable can be viewed as very slowly varying. This is equivalent to the relay feedback system with a slowly shifting hysteresis (Figure 26).

Setting $\gamma = 0$ (without loss of generality), gives a hysteresis for the new system that is not skewed[2].

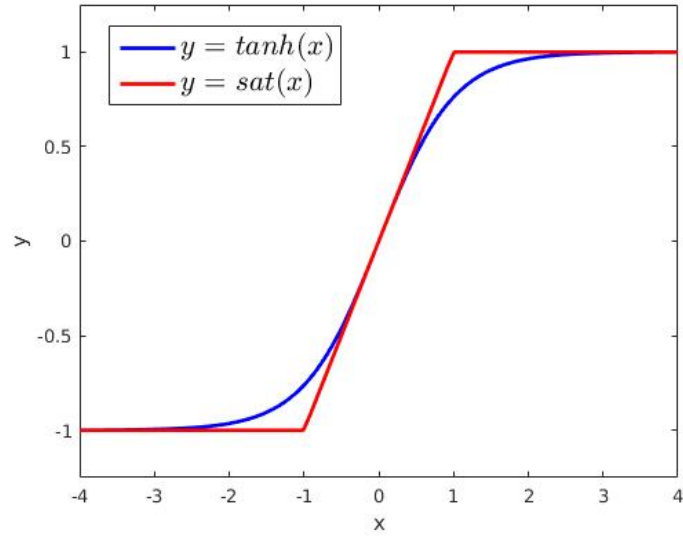[2]Transformation for skewed hysteresis was carried out in Section 3.2.2

Figure 21: The $S(\cdot)$ and the saturation functions. The saturation function is a good approximation to the $S(\cdot)$.
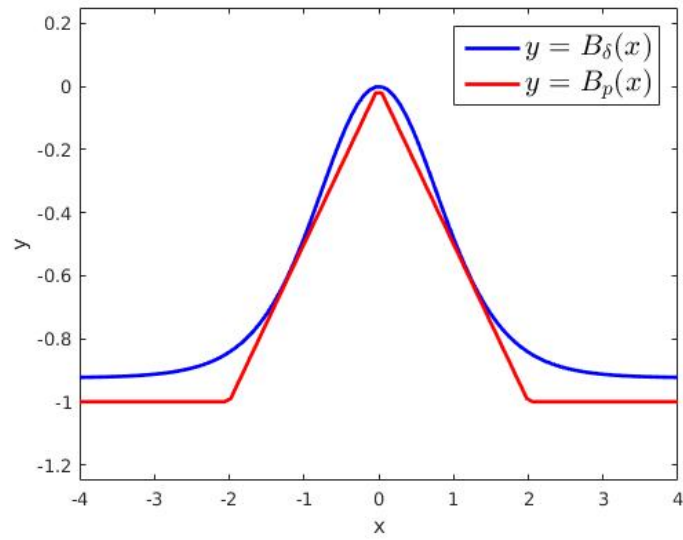

Figure 22: The $B_\delta(\cdot)$ with $\delta = 0.5$ and a piecewise linear approximation $B_p(\cdot)$.
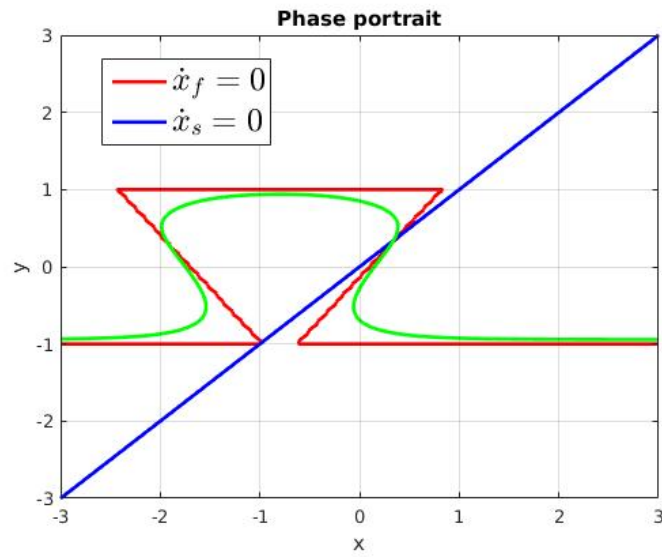
Figure 23: Phase portrait using piecewise-linear nonlinearities. The original fast nullcline is plotted in green for comparison. Note that the lines showing $\dot{x}_f = 0$ where $-1 < x_f < 1$ does not exist algebraicly. Numerical computing leads to those lines.
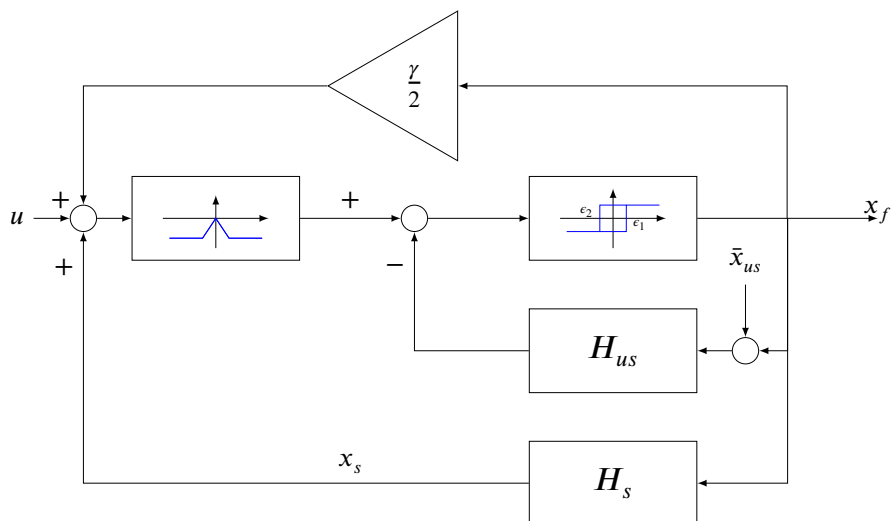

Figure 24: Inner loop replaced by relay with hysteresis. The hysteresis limits are $\epsilon_1 = \beta$ and $\epsilon_2 = \beta$.
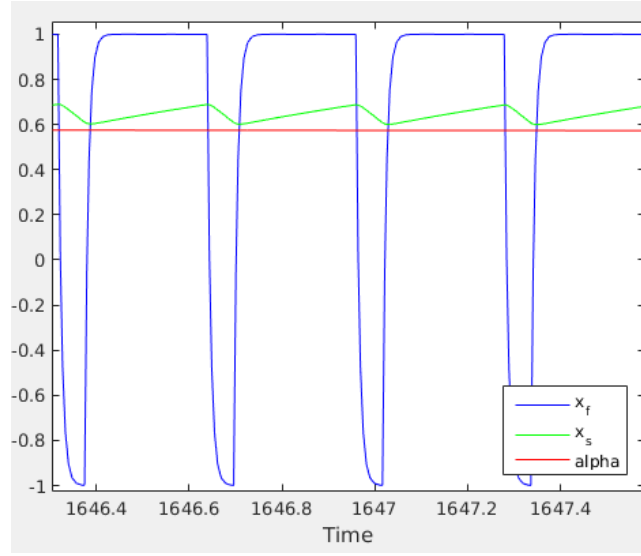
Figure 25: Variables changing during a very short period of spiking. The slow variable is adapting around the static hysteresis, like in the FitzHugh-Nagumo model. The utra slow variable is changing very slowly.
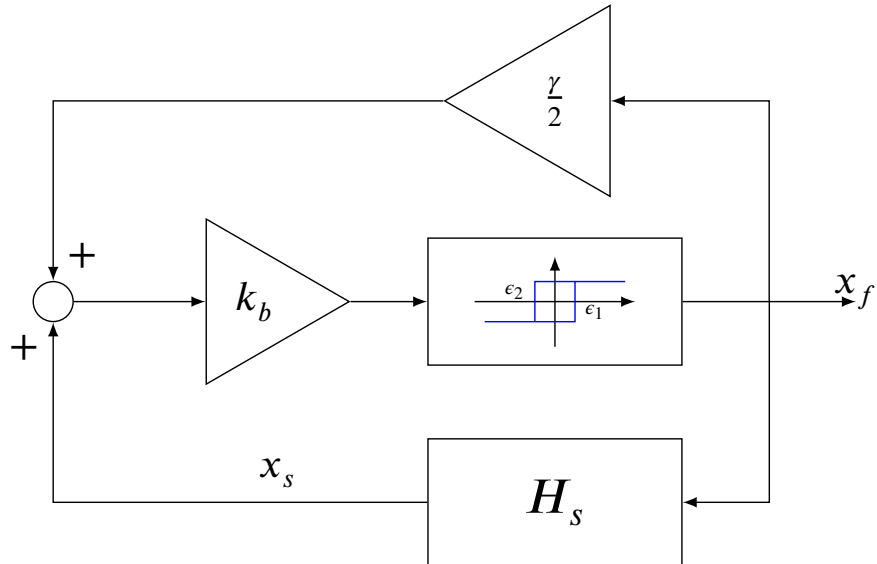

Figure 26: Relay feedback system with slowly shifting hysteresis. $\epsilon_1 = \beta - \alpha - k_b u$ and $\epsilon_2 = -\beta - \alpha - k_b u$
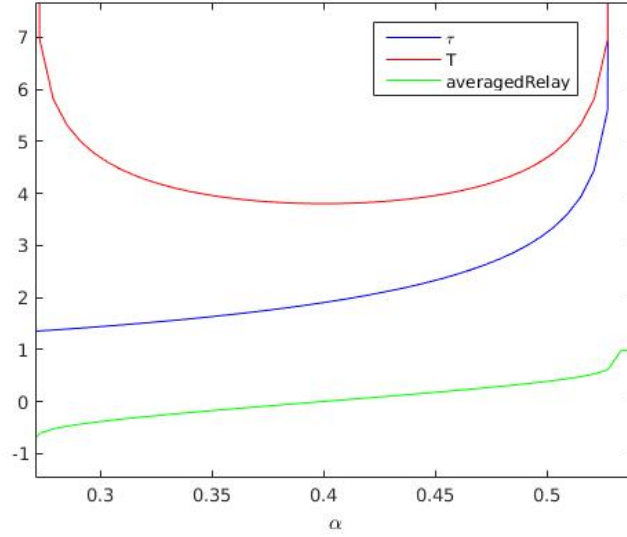
Figure 27: Duty cycle of the spiking oscillations changing with the ultra slow variable.
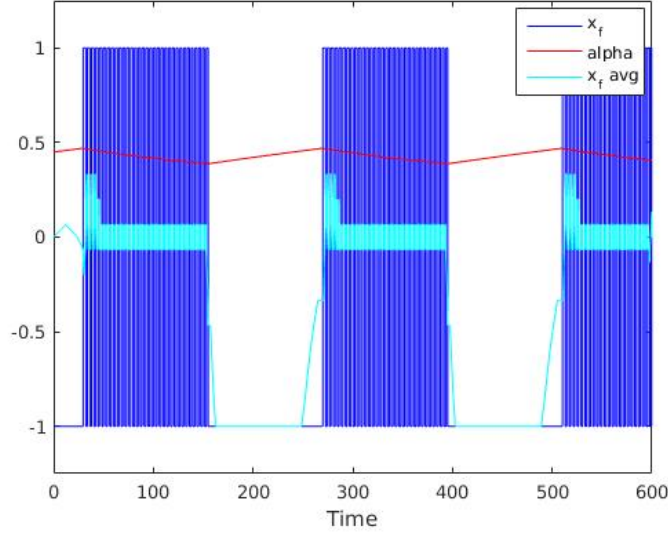

Figure 28: Moving average of x_f changes during spiking as α changes the hysteresis limits.

This allows us to use the analytical results from [5] to predict the time periods of the oscillations. The shifting hysteresis limits, due to the ultra slow variable, change the time periods of the oscillations as shown in Figure 27

The ultra-slow variable, due to its slow time constant, can be regarded as only responding to an "averaged" x_f. Figures 28 and 29 reveal the response of α to a moving average x_f. The relay hysteresis limit is the bistable range of α, while the maximum output of the relay can be roughly approximated as nearly zero. This reveals how the bursting circuit has been simplified into two coupled oscillators. The fast-slow oscillator which reproduces the spiking and the averge-fast–ultra-slow oscillator which dictates when the model spikes and rests (see Figure 30).

The transforming of the three time scale burster into relay feedback models now enables us to analytically extract the time period of the slow oscillation and that of the fast oscillation. It also
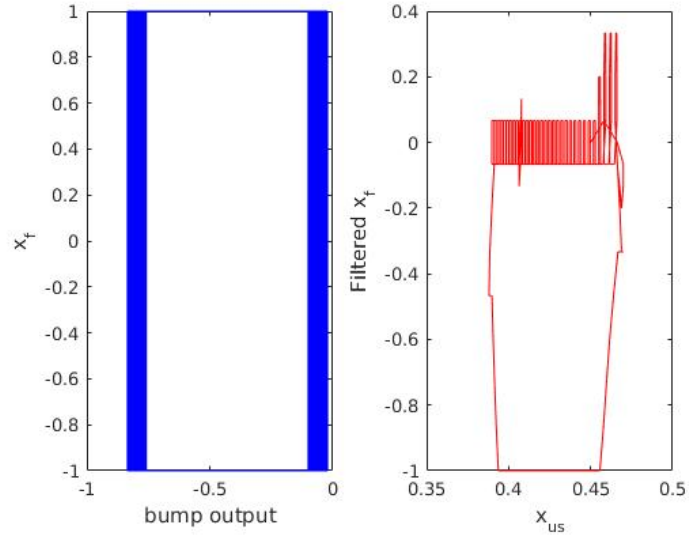
Figure 29: Trajectories on the phase plane reveal shifting hysteresis for x_f and an approximate relay hysteresis for α
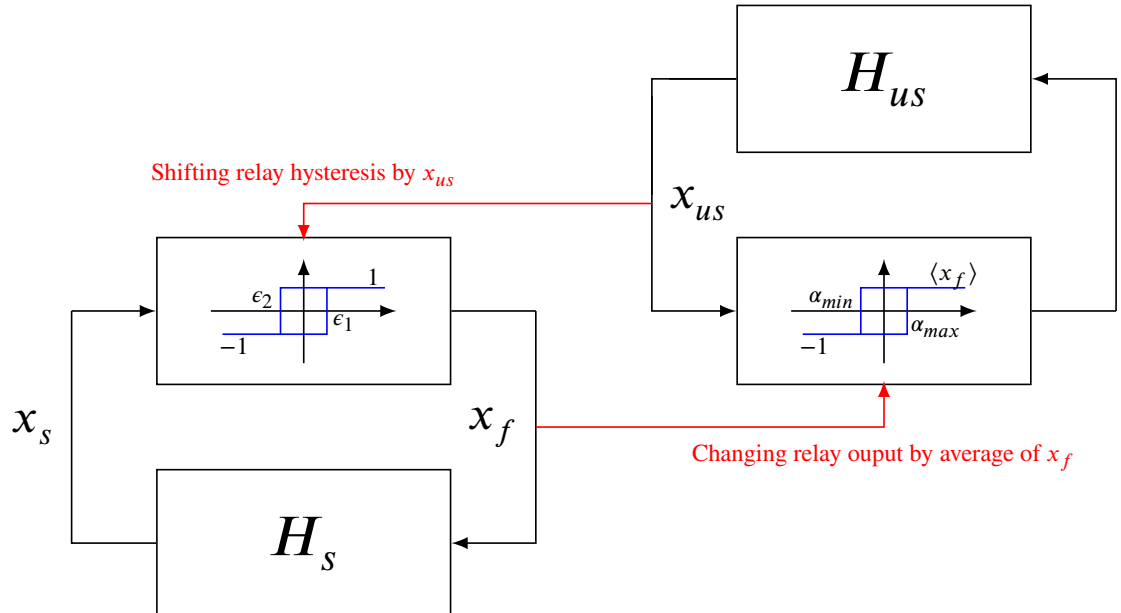

Figure 30: Coupled relay feedback system. The $\langle x_f \rangle$-x_{us} system affects the $x_f - x_s$ system by slowly shifting the hysteresis limits of the relay. The $x_f - x_s$ system affects the $\langle x_f \rangle$-x_{us} system by changing the magnitude of the relay ouput.

revealed how the two oscillators are linked and revealed how the duty cycle during spiking subtly changes due to the ultra-slow parameter.

4.3   Hindmarsh-Rose model

The method of breaking down bursting into two coupled relay feedback systems is a general approach. This section proves this by examining how a famous bursting model, the Hindmarsh-Rose model, can be described by two relay feedback systems.

4.3.1   Introduction

The Hindmarsh-Rose model provides one of the simplest models of the more general phenomenon of oscillatory burst discharge [15]. It is a slight modification of the FitzHugh-Nagumo model for action potentials, with an extra ultra-slow variable. It uses a parabolic nullcline for the slow variable instead of the a straight line and the equations are:

$$\epsilon_f \dot{x}_f = x_s - x_{us} + f(x_f) + I \tag{21}$$

$$\dot{x}_s = g(x_f) - x_s \tag{22}$$

$$\dot{x}_{us} = \tau_{us} \left(k(x_f - \bar{x}_{us}) - x_{us} \right) \tag{23}$$

$$\text{where } f(x) = 3x^2 - x^3 \text{ and } g(x) = 1 - 5x^2.$$

The fast variable, x_f, represents the membrane potential, the slow variable, x_s, is the current and x_{us} is the (ultra-slow) adaptation current. For bursting, the parameters used are $\tau_{us} = 0.001, k = 4, \bar{x}_{us} = 1.6, I = 2$. The behaviour of the model can be seen in Figure 31. The ϵ_f variable has been added to control the speed at which x_f adapts.

The Hindmarsh-Rose model has the same key features as the three-time scale bursting normal form (compare the block diagrams in Figure 16 and Figure 33). Both have a fast variable that is like the output of a relay with shifting hysteresis limits (see Figure 31a) as the ultra-slow variable adapts. The ultra-slow negative feedback modulates the shape of the fast nullcline to change the equilibrium positions (see Figure 32). The continous oscillations of the ultra-slow variable can be modelled as a relay.

The difference between this model and the three time scale bursting attractor model is that the latter places all the nonlinearities in the dynamics of x_f. The Hindmarsh-Rose model mirrors the nullcline of x_s by using a quadratic term, while the three time scale bursting attractor model mirrors the cubic nullcline using the bump nonlinearity.

4.3.2   Separation of time scales to separate into relay feedback systems

During spiking, the average of x_f is positive (see Figure 31. Since the slow plant is a low pass filter, we can assume that it only responds to the average of x_f. Consequently, similar to the 'bump', for the fast-slow system, the quadratic nonlinearity, $g(x_f)$, provides negative feedback, when spiking. When
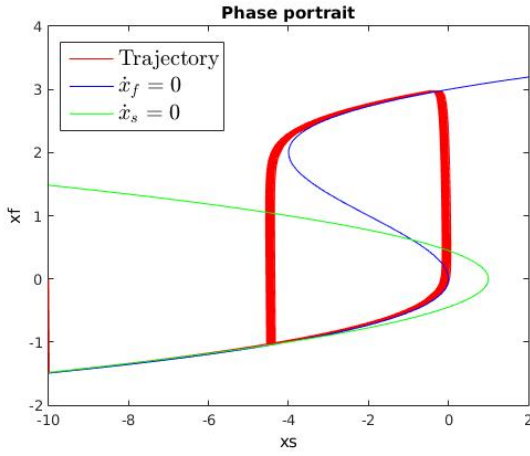
(a) Phase Portrait. Voltage is like the output of a skewed relay as $\epsilon_f \to 0$, just like in the FitzHugh-Nagumo model.
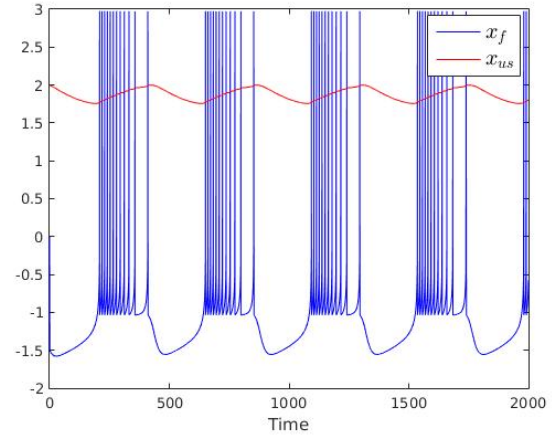
(b) Voltage oscillations against time. Voltage alternates between a high state and a low state when spiking. It then moves to a lower state while resting.
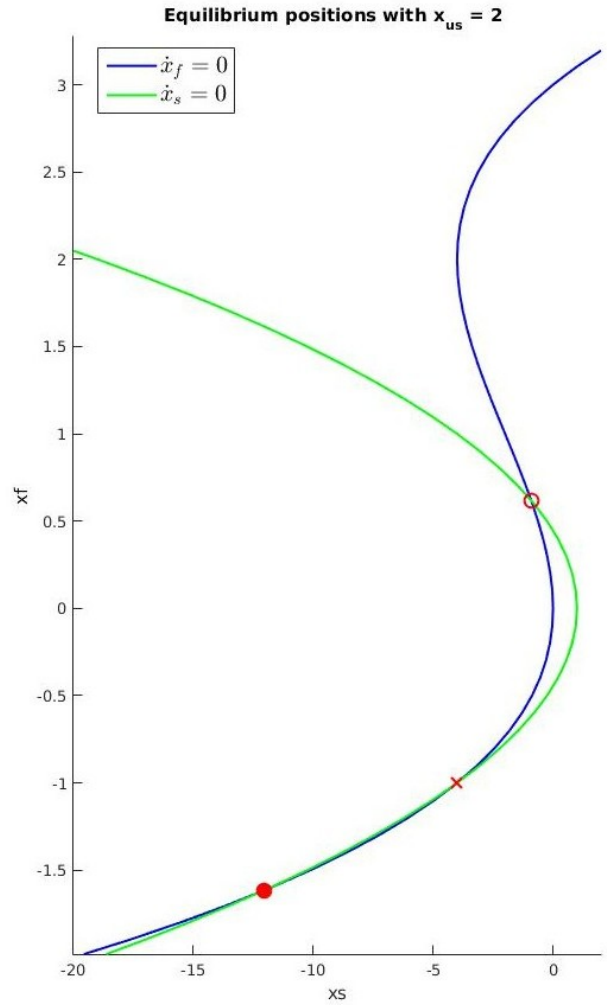
Figure 31: Hindmarsh-Rose model for bursting.

resting, the average x_f is negative and $g(x_f)$ provides positive feedback. This allows us to linearize the $g(x_f)$. The system is now identical to the FitzHugh-Nagumo model and can be modelled as a relay feedback system.

Following the same steps as described in the three time scale bursting normal form, the relay feedback model of the ultra-slow variable can be constructed. The relay would have a variable output, controlled by the average oscillations of the fast variable.
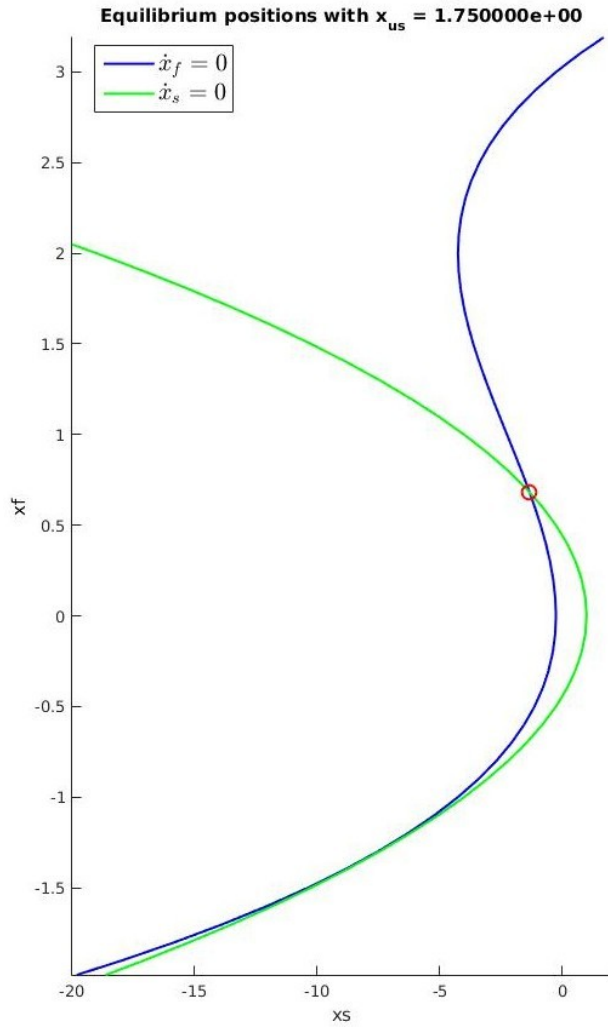
(a) The x_{us} is just small enough that the nullclines interesect only once. The system will switch to spiking as this happens.

(b) The x_{us} is just large enough that the nullclines interesect thrice. The system will switch to resting as this happens.

Figure 32: Fast nullcline of Hindmarsh-Rose model being modulated by the ultra-slow variable (x_{us}). Stable equilibrium is the filled circle, unstable equilibrium is the hollow circle and the saddle point is the cross. Between this range of x_{us}, the system is bistable.
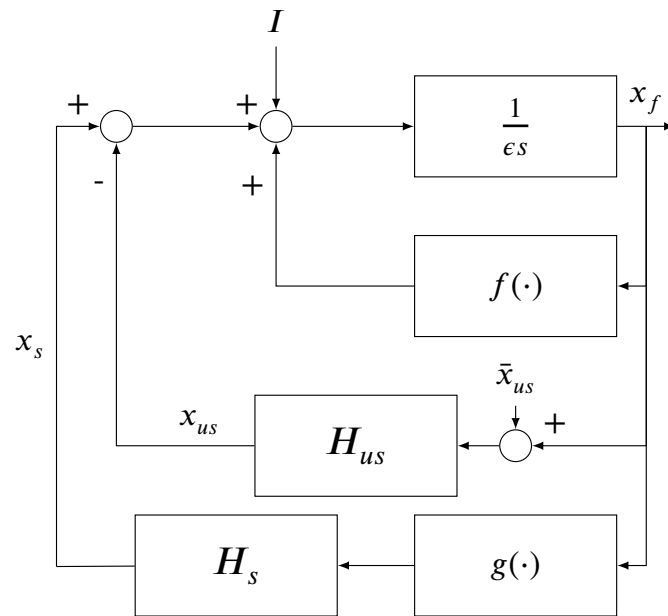
Figure 33: Hindmarsh-Rose model block diagram.

5 Conclusions

- Relay feedback systems were used to simulate different biological models, of increasing complexity.

- This framework provides tools using which the effect of parameters can be understood.

- It is able to predict the existence of oscillations and their time periods. This is a step towards answering the question from [13]: How robust is the bursting mechanism to parameter variations in the physiological range?

- However, this framework fails to caputure the excitatory nature of models. Relay feedback systems are not excitable systems, they are only oscillatory systems.

- Future work would involve perhaps modelling the next level of nested oscillations. This could perhaps be generalised to an Nth level nested oscilaltions. This would then relate back to engineering systems with multirate feedback systems.

6 Acknowledgements

References

[1] C.P.Fall, E.S.Marland, J.M.Wagner, J.J.Tyson, *Computational Cell Biology*. Springer. Volume 20. ISBN 0-387-95369-8.

[2] A.Goldbeter. (2002). *Computational approaches to cellular rhythms.* Nature, Voluem 420, Pages 238-245.

[3] A.Goldbeter and M.J.Berridge. (1996). *Biochemical oscillations and cellular rhythms.* Cambridge University Press, ISBN 9780511608193.

[4] C.C.Hang, K.J.Åström, Q.G.Wang, (2002) *Relay feedback auto-tuning of process controllers — a tutorial review.* Journal of Process Control, Volume 12, Pages 143-162.

[5] K.J.Åström , (1995) *Oscillations in systems with relay feedback.* IMA Vol. Math. Appl. : Adap. Control, Filtering, Signal Processing, Volume 74, Pages 1-25.

[6] J.Keener and J.Sneyd, *Mathematical Physiology*. Springer-Verlag New York. Volume 8/I. Second Edition. ISBN 978-0-387-75846-6.

[7] J.C.Leloup and A.Goldbeter. (1998). *A model for circadian rhythms in Drosophila incorporating the formation of a complex between PER and TIM proteins*. J.Biol.Rhythms, Volume 13, Pages 70-87.

[8] A.Hodgkin and A.Huxley. (1952). *A quantitative description of membrane current and its application to conduction and scitation in nerve*. J. Physiol, Volume 117, Pages 500-544.

[9] R.FitzHugh. (1961). *Impulses and physiological states in theoretical models of nerve membrane*. Biophysical Journal, Volume 1, Pages 445-466.

[10] G.C.Goodwin, S.F.Graebe, M.E.Salgado, (2000). *Control System Design*. Prentice Hall, ISBN 978-0-13-958653-8.

[11] A.Franci and R.Sepulchre, (2014). *Realization of nonlinear behaviours from organizing centers*. Proc. 53st. IEEE Conf. Decision Contr., Pages 56-61.

[12] A.Franci, G.Drion and R.Sepulchre, (2014). *Modeling the modulation of neuronal bursting: a singularity theory approach*. SIAM Journal of Applied Dynamical Systems, Volume 13, Pages 798-829.

[13] J.Rinzel. (1986). *A formal classification of bursting mechanisms in excitable systems.*, Proc. Int. Cong. Mathematicians, Berkeley, California, USA.

[14] G.Drion, T.O'Leary, J.Dethier, A.Franci and R.Sepulchre. (2015) *Neuronal behaviors: a control perspective*. 54th IEEE Conference on Decision and Control, Osaka, Japan, Pages 1923-1944. Tutorial paper.

[15] J.L.Hindmarhs and R.M.Rose, (1984). *A model of neuronal bursting using three coupled first order fifferential euations*, Proc. R. Soc. Lond., Volume 221, Pages 87-102.

[16] G.M.Kranc. (1957). *Input-output analsis of multirate feedback systems*. IRE Transactions on Automatic Control, Volume 3, Pages 21-28.

Appendices

A Local stability relay model of Goodwin oscillator

To check the local stability of the relay model of the Goodwin oscillator, we use Theorem 5.2 from [5]. It requires that the eigenvalues of the W matrix lies within the unit disc. The matrix is defined as:

$$W = \left(I - \frac{w_2 C}{C w_2} \right) \Phi_2 \left(I - \frac{w_1 C}{C w_1} \right) \Phi_1 \tag{24}$$

where

$$w_1 = \Phi_1 (A a_1 + B d_1) \tag{25}$$

$$w_2 = \Phi_2 (A a_2 - B d_2) \tag{26}$$

$$a_1 = (I - \Phi)^{-1} (\Phi_2 \Gamma_1 d_1 - \Gamma_2 d_2) \tag{27}$$

$$a_2 = (I - \Phi)^{-1} (-\Phi_1 \Gamma_2 d_2 + \Gamma_1 d_1) \tag{28}$$
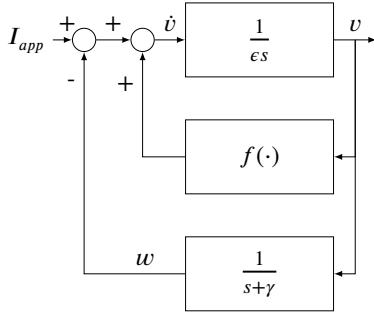
$$\tag{29}$$

and as defined in Section 2.2

$$\Phi = e^{AT} , \Phi_1 = e^{A\tau} , \Phi_2 = e^{A(T-\tau)}$$
$$\Phi_1 = \int_0^\tau e^{As} \mathrm{d}s\, B , \Gamma_2 = \int_0^{T-\tau} e^{As} \mathrm{d}s\, B \tag{30}$$

For our model, the oscillation is split such that $\tau = 0.19s$ and $T = 5.93s$. With A, B, C defined by **??**, we get that:
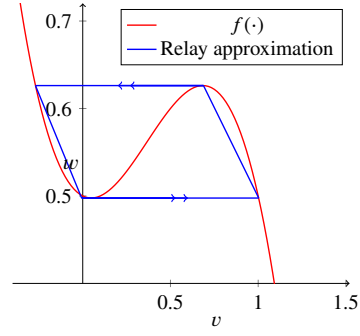
$$W = 10^{-2} \begin{bmatrix} -2.0 & -3.1 & -8.6 \\ -5.6 & -8.8 & -24.2 \\ 0.0 & 0.0 & 0.0 \end{bmatrix} \tag{31}$$

which has eigenvalues $-7.9 \times 10^{-6}, -1.1 \times 10^{-2}$ and 0. Hence the limit cycle is locally stable.

B   FitzHugh-Nagumo to standard relay feedback

(a) Block diagram

(b) Nonlinearity and the "relay" approximation
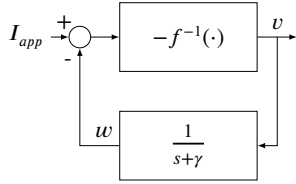
Figure A1: FitzHugh-Nagumo
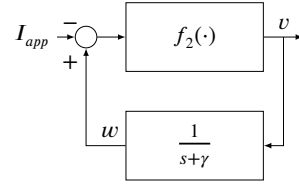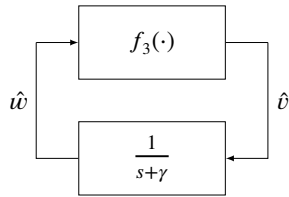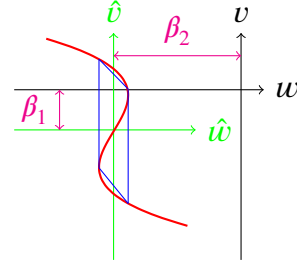

Figure A2: High gain inversion

Figure A3: $f_2(x) = -f^{-1}(-x)$

(a) Block diagram

(b) Nonlinearity in new co-ordinates, $f_3(\cdot)$

Figure A4: Shift co-ordinate system to make relay symmetric, I_{app} disappears. $\hat{w} = w + \beta_2$ and $\hat{v} = v + \beta_1$
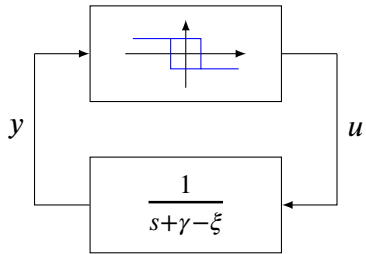

Figure A5: Change of basis to use relay. $\hat{w} = y$ and $\hat{v} = \xi y + u$

Following the steps from the Figures A1 to A5 allow the standard relay to be used to model the FitzHugh-Nagumo equations. The original variables can be recovered as:

$$\begin{cases} v = \hat{v} - \beta_1 = \xi y + u - \beta_1 \\ w = \hat{w} - \beta_2 = y - \beta_2 \end{cases}$$

The first step in replacing the cubic nullcline was to approximate it using a skewed relay. This involved selecting four points on the nullcline that represented the essential behaviour. The points chosen were:

$$(-0.2693, 0.6262), (0.6883, 0.6262), (-0.0061, 0.4976), (1.003, 0.4976) \tag{32}$$

These points now represent the nonlinear function $f(v)$. They undergo the transformations described in the above figures in order to convert them to a standard relay feedback system. To inverse the $f(v)$, each point was reflected about the $y = x$ line. Then they were reflected about the x-axis in order to swap the signs of the input signals. Next, they were reflected in the y-axis due to the minus sign. To centralise the relay about the origin, they points were shifted by $(\beta_2, \beta_1) = (-0.562, -0.354)$. ξ was then chosen in order to get a standard relay — multiply each point by the matrix S,:

$$S = \begin{bmatrix} 1 & 0 \\ -\xi & 1 \end{bmatrix} = \begin{bmatrix} 1 & 0 \\ 2 & 1 \end{bmatrix} \tag{33}$$

This resulted in the four points being positioned at:

$$(0.0643, 0.4917), (0.0643, -0.4917), (-0.0643, 0.4917), (-0.0643, -0.4917) \tag{34}$$

The skew matrix can be understood by considering the skewed relay as simply a relay with an extra loop as shown below. The equations show where the skew matrix comes from. Lumping the extra loop with the original plant gives the new system.
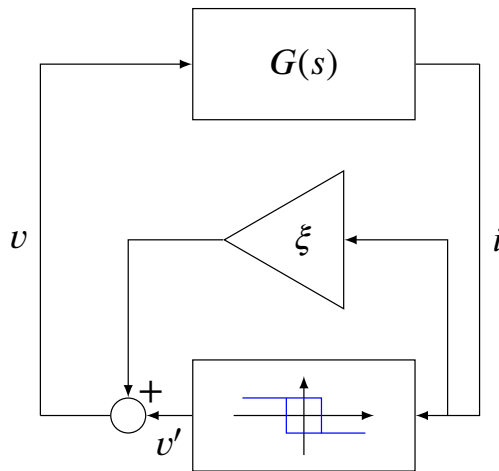

Figure A6: Skewed relay

$$i = G(s)v \tag{35}$$

$$v = \xi i + v' \tag{36}$$

we want i in terms of v' \hfill (37)

$$i = G(s)(\xi i + v') \tag{38}$$

$$i = \left(\frac{G(s)}{1 - \xi G(s)} \right) v' \tag{39}$$

$$G(s) = \frac{1}{s + \gamma} \tag{40}$$

$$\Rightarrow i(s) = \left(\frac{1}{s + \gamma - \xi} \right) v'(s) \tag{41}$$

This is a standard relay with hysteresis limits $\epsilon = 0.0643$ and output $d = 0.4917$. The state-space representation of this system was thus:

$$\dot{x} = (\gamma - \xi)x + u = 2.5x + u \tag{42}$$

$$y = x \tag{43}$$

$$u = \begin{cases} -0.4917 \text{ if } e > 0.0643 \text{ or } (e > -0.0643 \text{ and } u(t-) = 0.4917) \\ 0.4917 \text{ if } e < -0.0643 \text{ or } (e < 0.0643 \text{ and } u(t-) = -0.4917) \end{cases} \tag{44}$$

The original system is then recovered by:

$$v = \xi y + u - \beta_1 = -2y + u + 0.354 \tag{45}$$

$$w = y - \beta_2 = y + 0.562 \tag{46}$$

Using equation **??**, the time period was predicted to be 0.54 seconds. The local stability was tested using Theorem 3.1 of [5], with the W matrix being equal to zero and hence having eigenvalues within the unit disk.

C Three time scale burster

In order to find the bistable range for the piece-wise linear model of the system, it requires us to find the two critical points at which the system changes from having only one equilibrium to two equilibriums. This was shown for the original model in Figure **??**.

The fast nullcline can be written as:

$$G(x_f, x_s, \alpha) = -x_f + \text{sign} \left(B \left(u + x_s + \tfrac{1}{2}\gamma x_f \right) + \beta x_f + \alpha \right) \tag{47}$$

The extreme point of the lower branches are right when the sign $(\cdot)$ function changes from being 1 to
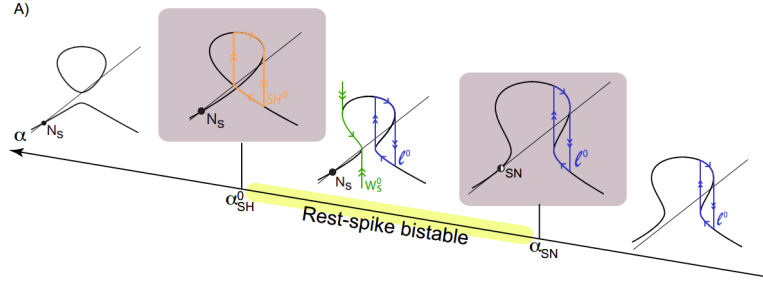
Figure A7: The bistable range for the α parameter.

-1. Since $x_f = -1$, this means: $B(u + x_s - \frac{1}{2}\gamma) - \beta + \alpha = 0$. This can be written as:

$$\frac{1}{2}(u + x_s - \frac{1}{2}\gamma) - \beta + \alpha = 0 \qquad \text{if} -2 < (u + x_s - \frac{1}{2}\gamma) < 0 \qquad (48)$$

$$-\frac{1}{2}(u + x_s - \frac{1}{2}\gamma) - \beta + \alpha = 0 \qquad \text{if} \ 0 < (u + x_s - \frac{1}{2}\gamma) < 2 \qquad (49)$$

$$(50)$$

We are first concerned at which point the linear nullcline intersects the lower left hand branch of the fast nullcline. At that point, $x_f = -1$. This implies that $x_s = -1$ as well. This means:

$$\alpha_{max} = \beta + \frac{1}{2}(u - 1 - \frac{1}{2}\gamma) \qquad (51)$$

The two extreme points of the lower branch meet when we reach the peak of the bump, i.e $u + x_s - \frac{1}{2}\gamma = 0$. Thus:
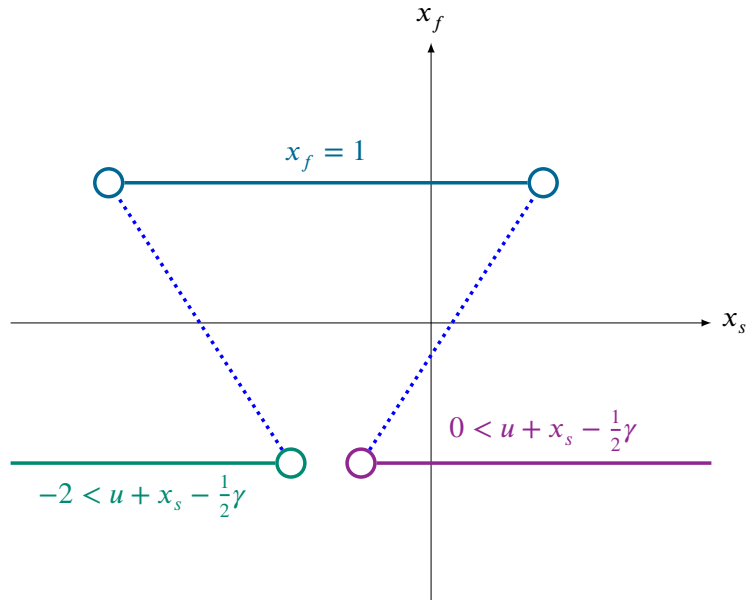
$$\alpha_{min} = \beta \qquad (52)$$

Figure A8: Fast nullcline branches.

D   Risk assessment retrospective

This project was research oriented and involved using MATLAB and Simulink in order to simulate different models. The only risks were those associated with working on a computer for extended periods of time. This was as expected at the onset of the project. Taking regular breaks and good posture helped to reduce the risks.